JOURNAL OF THERMOPHYSICS AND HEAT TRANSFER
Vol. 25, No. 4, October–December 2011

Technical Notes

Numerical Uncertainty for Radiative Transfer Equation by an Information Entropy Approach

H.-C. Zhang,* Y. Li,† and H.-P. Tan‡
Harbin Institute of Technology, 150001 Harbin, People's Republic of China

DOI: 10.2514/1.T3630

Downloaded by HARBIN INSTITUTE OF TECHNOLOGY on April 22, 2014 | http://arc.aiaa.org | DOI: 10.2514/1.T3630

Nomenclature

f	=	spatial differencing factor
H	=	information entropy indicator, bit
$I_{b\lambda}$	=	blackbody spectral radiative intensity, $\mathrm{W/(m^2\text{-}sr\text{-}\mu m)}$
I_λ	=	spectral radiative intensity, $\mathrm{W/(m^2\text{-}sr\text{-}\mu m)}$
i, j	=	index of nodal point in the region without laser incidence
NX	=	spatial discretization grid number along x axis
NY	=	spatial discretization grid number along y axis
$N\theta$	=	angular discretization grid number along θ direction
$N\varphi$	=	angular discretization grid number along φ direction
$\mathbf{n}_b$	=	normal vector of the boundary
p	=	probability of temperature increasing due to numerical scattering
$\mathbf{s}$	=	spatial position vector, m
T	=	temperature, K
γ	=	transmittance
ε	=	emissivity
$\kappa_{a\lambda}$	=	spectral absorption coefficient of medium, $\mathrm{m^{-1}}$
$\kappa_{s\lambda}$	=	spectral scattering coefficient of medium, $\mathrm{m^{-1}}$
λ	=	wavelength, μm
τ	=	optical thickness
Φ	=	scattering-phase function
$\mathbf{\Omega}$	=	solid-angle ordinate direction
$\mathbf{\Omega}'$	=	solid-angle ordinate for scattering direction

Subscripts

b	=	bottom boundary of control volume p
e	=	east boundary of control volume p
i, j	=	index of nodal point in the region without laser incidence
n	=	north boundary of control volume p
p	=	control volume p
s	=	south boundary of control volume p
t	=	top boundary of control volume p
w	=	west boundary of control volume p
x, y, z	=	coordinates directions
λ	=	spectrum (wavelength)
0	=	initial value

Superscript

Ω^l	=	a certain selected angular direction

Received 20 September 2010; revision received 21 May 2011; accepted for publication 23 May 2011. Copyright © 2011 by the American Institute of Aeronautics and Astronautics, Inc. All rights reserved. Copies of this paper may be made for personal or internal use, on condition that the copier pay the $10.00 per-copy fee to the Copyright Clearance Center, Inc., 222 Rosewood Drive, Danvers, MA 01923; include the code 0887-8722/11 and $10.00 in correspondence with the CCC.

*Lecturer, School of Energy Science and Engineering & Institute of Composite Material, Heilongjiang Province; zhc5@vip.163.com, Member AIAA.

†Professor, Institute of Composite Material, Heilongjiang Province; liyao@hit.edu.cn (Corresponding Author).

‡Professor, School of Energy Science and Engineering, Heilongjiang Province; tanheping@hit.edu.cn.

I. Introduction

RADIATIVE heat transfer plays a very important role in many scientific and engineering applications [1]. The general equation to describe its transport process is the radiative transfer equation (RTE). Up to now, several approximate methods have been developed for solution of the RTE, and among them, the finite volume method (FVM) has proven to be an efficient algorithm [2]. Recently, it has been applied to various complicated problems, as is shown in [3–7].

For any numerical method, uncertainty is an important and integral part in connection with the solution procedures; and essentially, FVM will encounter different errors when it is applied to investigate radiative heat transfer problems. The most common uncertainty that occurs is the so-called false scattering, which was initially identified by Chai et al. [8] in the discrete ordinate method (DOM). However, in many respects, FVM is similar to DOM, since the RTE is also solved through a set of algebraic equations that is obtained by discretizing the control equation over user-selected control volumes and specific control solid angles. It has been shown that many factors can cause uncertainty [9] influencing solution accuracy, including spatial discretization scheme [10], grid resolution [11], radiative properties [12], and volumetric heat sources [13]. However, there are few effective routines for analyzing and evaluating the uncertainties.

The concept and theory of entropy, based on the second law of thermodynamics, has been an innovative and effective approach to studying computational errors within the fields of fluid flow and heat transfer [14]. The traditional theory of entropy production is used to analyze numerical errors for viscous compressible flow [15]. The concept of information entropy [16] has been shown to be an appropriate method and has been widely applied to error analysis for Euler's equations and the stability of numerical solution [17]. In radiative transfer, although some work has been done based on radiation entropy generation [18,19], much work has been focused on error analysis in computational fluid dynamics, conduction, and convection, instead of error analysis for radiative transfer.

In this Note, physical models of normal and oblique laser incidence are used as basic benchmark schemes, in addition to using reference data from the Monte Carlo method (MCM), which has been proven to generate no false scattering [9]. An entropy formula based on information theory [16] is proposed to investigate uncertainty in FVM during the solution procedure. Information entropy values for spatial discretization schemes, angular discretization numbers, spatial grid numbers and radiative properties will be evaluated.

II. Physical Models and Information Entropy Formula

In a participating medium, the RTE can be expressed as

$$\frac{\mathrm{d}I_\lambda(\mathbf{s},\mathbf{\Omega})}{\mathrm{d}s} = -\kappa_{a\lambda} I_\lambda(\mathbf{s},\mathbf{\Omega}) - \kappa_{s\lambda} I_\lambda(\mathbf{s},\mathbf{\Omega}) + \kappa_{a\lambda} I_{b\lambda}(\mathbf{s}) + \frac{\kappa_{s\lambda}}{4\pi}\int_{4\pi} I_\lambda(\mathbf{s},\mathbf{\Omega}')\Phi_\lambda(\mathbf{\Omega}',\mathbf{\Omega})\,\mathrm{d}\Omega' \tag{1}$$

For an oblique, diffuse emitting, and reflective boundary wall, the corresponding boundary condition can be written as

$$I_\lambda(\mathbf{\Omega}) = \varepsilon_\lambda I_{b\lambda} + \frac{1-\varepsilon_\lambda}{\pi}\int_{\mathbf{n}_b\cdot\mathbf{\Omega}'<0} I_\lambda(\mathbf{\Omega}')|\mathbf{n}_b\cdot\mathbf{\Omega}'|\,\mathrm{d}\mathbf{\Omega}' \qquad (2)$$

When FVM is used to solve the RTE, hemispherical space of 4π sr is divided to a solid-angle grid, i.e., a limited number of directions. Along a specific direction Ω^l, a relationship is usually taken to correlate the radiative intensities at the face of the control volume to the intensities at the center of control volume. This yields a spatial differencing scheme, which, in general, can be represented as

$$I_p^{\Omega^l} = f_x I_e^{\Omega^l} + (1-f_x)I_w^{\Omega^l} + f_y I_n^{\Omega^l} + (1-f_y)I_s^{\Omega^l} + f_z I_t^{\Omega^l} + (1-f_z)I_b^{\Omega^l} \qquad (3)$$

where different values for f_x, f_y, and f_z correspond to different types of differencing schemes.

Frequently, the following three kinds of differencing schemes are selected, namely, the step scheme with $f_x = f_y = f_z = 1.0$, the diamond scheme with $f_x = f_y = f_z = 0.5$, and the exponential scheme with

$$f_x = [1-\exp(-\tau_x^{\Omega^l})]^{-1} - (\tau_x^{\Omega^l})^{-1} \qquad (4)$$

$$f_y = [1-\exp(-\tau_y^{\Omega^l})]^{-1} - (\tau_y^{\Omega^l})^{-1} \qquad (5)$$

$$f_z = [1-\exp(-\tau_z^{\Omega^l})]^{-1} - (\tau_z^{\Omega^l})^{-1} \qquad (6)$$

where τ is the optical thickness.

To access the numerical uncertainty, artificial physical models such as a two-dimensional rectangle containing a participating medium with normal and oblique laser incidence are adopted (see Figs. 1 and 2). Detailed information on these two models can be found in [9,12].

According to the definition of information entropy [16], an error indicator can be defined as

$$H = -\sum_{i,j} p(i,j)\log_2[p(i,j)] \qquad (7)$$

where $p(i,j)$ is the probability of temperature increasing due to numerical scattering, if any, in the region without laser incidence, according to specific temperature ranges.

To obtain information entropy, the RTE is first solved by FVM, and temperature distribution is also obtained. In the region without laser incidence, the following expression for temperature increment is defined:

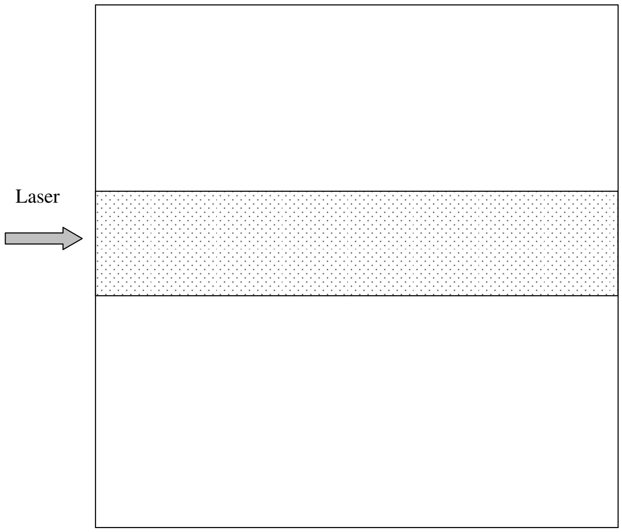

Fig. 1 Physical model of normal laser incidence on a two-dimensional participating medium.

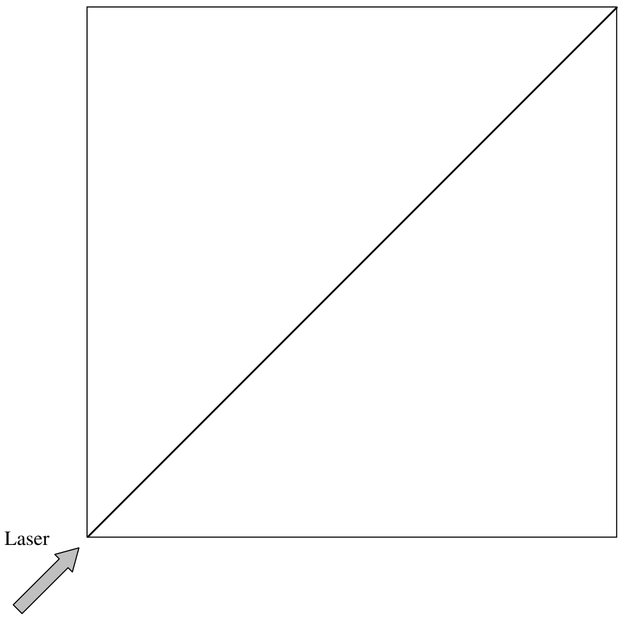

Fig. 2 Physical model of oblique laser incidence on a two-dimensional participating medium.

$$\Delta T_{i,j} = T_{i,j} - T_0 \qquad (i,j \notin \text{laser incidence}) \qquad (8)$$

Since there are a number of $\Delta T_{i,j}$ values, they should be arranged by different ranges, and in the current study, all of the $\Delta T_{i,j}$ values are sorted to three ranges, i.e.,

$$[0, \min(\Delta T_{i,j})], \qquad \left[\min(\Delta T_{i,j}), \frac{\min(\Delta T_{i,j}) + \max(\Delta T_{i,j})}{2}\right] \left[\frac{\min(\Delta T_{i,j}) + \max(\Delta T_{i,j})}{2}, \max(\Delta T_{i,j})\right]$$

Then the probability of temperature increasing or falling into a specific range can be determined. Furthermore, all of probabilities can be summed over all grid points according to Eq. (7).

III. Results and Discussion

In the following example, radiative properties and other computing parameters are the same as those in [12], i.e., $\kappa_{a\lambda} = 1\ \mathrm{m}^{-1}$ and $\kappa_{s\lambda} = 0$; emissivities of the four interfaces are all 0.8, with $\lambda = 10.6\ \mu\mathrm{m}$, $\varepsilon_w = 0$, and $\gamma_w = 0.8$. In addition, temperature increment ranges are set according to the results from FVM calculations.

For the MCM, the information entropy H values for the cases of $NX \times NY = 5\times5$, 10×10, and 20×20 are equal to 0.0. As a statistical method, MCM has high accuracy, which suffers no numerical uncertainty caused by spatial and angular discretization numbers. In this sense, it has the minimum H value, the results of which can be adopted as the reference data for evaluating the uncertainties of FVM. In addition, to see that the results are independent of grid number, results in [9] can be reviewed in order to see verification of the computational program and the effect of grid number for unit optical thickness.

H values for different angular discretization and spatial grid values for FVM in the cases of normal laser incidence and oblique laser incidence are shown in Tables 1 and 2, respectively. It can be seen that the uncertainty for FVM is affected by the interplay of angular discretization and spatial grid values simultaneously; i.e., if a higher accuracy is expected for FVM, a good compromise between both kinds of value is necessary. With increasing grid values, H decreases, which means fewer errors are generated.

Table 3 and 4 display H values for different spatial discretization schemes, with **a** fixed $N\theta \times N\varphi$ of 20×28 for different spatial grid values, in the cases of normal laser incidence and oblique laser incidence, and for the step scheme (FVM1), diamond scheme

Downloaded by HARBIN INSTITUTE OF TECHNOLOGY on April 22, 2014 | http://arc.aiaa.org | DOI: 10.2514/1.T3630

Downloaded by HARBIN INSTITUTE OF TECHNOLOGY on April 22, 2014 | http://arc.aiaa.org | DOI: 10.2514/1.T3630

Table 1 ***H*** **values for different angular discretization and spatial grid values in the case of normal laser incidence**

	$N\theta \times N\varphi$					
$NX \times NY$	4×8	10×12	12×16	16×20	20×28	24×36
5×5	1.0	0.9927	0.9712	0.8813	0.7219	0.7219
10×10	0.9183	0.9641	0.8524	0.6503	0.5033	0.4690
20×20	0.7668	0.7425	0.6892	0.6293	0.4855	0.2975

Table 2 ***H*** **values for different angular discretization and spatial grid values in the case of oblique laser incidence**

	$N\theta \times N\varphi$					
$NX \times NY$	4×8	10×12	12×16	16×20	20×28	24×36
5×5	1.0	0.8736	0.8595	0.7844	0.6497	0.6533
10×10	0.8357	0.8870	0.7885	0.6048	0.4731	0.4432
20×20	0.7055	0.6853	0.6368	0.5802	0.4471	0.2755

Table 3 ***H*** **values for different spatial discretization schemes in the case of normal laser incidence[a]**

$NX \times NY$	FVM1	FVM2	FVM3	MCM
5×5	0.7219	0.7219	0.7219	0.0
10×10	0.5033	0.6641	0.6183	0.0
20×20	0.4855	0.6315	0.5638	0.0

[a]FVM1 for step scheme, FVM2 for diamond scheme, and FVM3 for exponential scheme.

Table 4 ***H*** **values for different spatial discretization schemes in the case of oblique laser incidence[a]**

$NX \times NY$	FVM1	FVM2	FVM3	MCM
5×5	0.6497	0.6497	0.6497	0.0
10×10	0.4731	0.5982	0.5502	0.0
20×20	0.4471	0.5723	0.5274	0.0

[a]FVM1 for step scheme, FVM2 for diamond scheme, and FVM3 for exponential scheme.

(FVM2), and exponential scheme (FVM3). It can be seen that the degree of uncertainty from best to worst is FVM2, FVM3, and FVM1, i.e., the diamond scheme, the exponential scheme, and the step scheme.

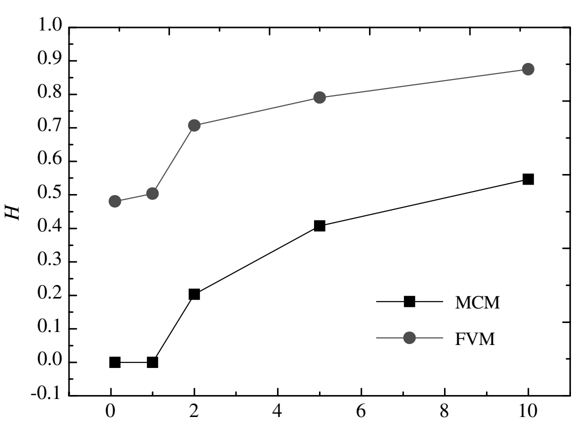

Fig. 3 ***H*** **values for different absorption coefficients by MCM and FVM in the case of normal laser incidence.**

When $\kappa_{\alpha\lambda}$ is chosen to be 0.1, 1.0, 2.0, 5.0, and 10.0, with $NX \times NY = 10 \times 10$ and $N\theta \times N\varphi = 20 \times 28$, for MCM and FVM in the case of normal laser incidence, H is computed as shown in Fig. 3. In the case of oblique laser incidence, the trends are similar, so that figure has been omitted for brevity.

It can be seen that for $\kappa_{\alpha\lambda}$ varying from 0.1 to 1.0, there is small variation in H and when $\kappa_{\alpha\lambda} > 0.1$, H has an abrupt change. Although there is some change for oblique laser incidence, the trends are almost the same.

IV. Conclusions

Based on the definition of information entropy, an error indicator H is defined to evaluate and compare uncertainties caused by different factors in FVM for solving the RTE, which is proven to be an effective approach. MCM has the minimum values for H, which indicates that it suffers minimum uncertainty caused by spatial and angular discretization values. The information entropy indicator also shows that the uncertainty for FVM is affected by the interplay of angular discretization and spatial grid values simultaneously. H is also affected by different spatial discretization schemes to a large degree. In addition, information entropy is also affected by the spatial discretization scheme, with the diamond scheme being best, then the exponential scheme and step scheme, in rank order. Information entropy also varies with the amount of absorption, which can produce a large degree of uncertainty.

Acknowledgments

The work described herein is supported by the National Natural Science Foundation of China (nos. 51006026 and 90916020), and this project was also supported by the Development Program for Outstanding Young Teachers in Harbin Institute of Technology (no. HITQNJS.2009.022), to whom grateful acknowledgment is expressed.

References

[1] Siegel, R., and Howell, J. R., *Thermal Radiation Heat Transfer*, 4th ed., Taylor & Francis, New York, 2002.

[2] Raithby, G. D., and Chui, E. H., "A Finite-Volume Method for Predicting a Radiant Heat Transfer in Enclosures with Participating Media," *Journal of Heat Transfer*, Vol. 112, 1990, pp. 415–423. doi:10.1115/1.2910394

[3] Borjini, M. N., Guedri, K., and Said, R., "Modeling of Radiative Heat Transfer in 3D Complex Boiler with Non-Gray Sooting Media," *Journal of Quantitative Spectroscopy and Radiative Transfer*, Vol. 105, No. 2, 2007, pp. 167–179. doi:10.1016/j.jqsrt.2006.11.001

[4] Das, R., Mishra, S. C., Ajith, M., and Uppaluri, R., "An Inverse Analysis of a Transient 2-D Conduction-Radiation Problem Using the Lattice Boltzmann Method and the Finite Volume Method Coupled with the Genetic Algorithm," *Journal of Quantitative Spectroscopy and Radiative Transfer*, Vol. 109, No. 11, 2008, pp. 2060–2077. doi:10.1016/j.jqsrt.2008.01.011

[5] Bazdidi-Tehrani, F., and Shahini, M., "Combined Mixed Convection-Radiation Heat Transfer Within a Vertical Channel: Investigation of Flow Reversal," *Numerical Heat Transfer, Part A, Applications*, Vol. 55, No. 3, 2009, pp. 289–307. doi:10.1080/10407780802628912

[6] Han, S. H., Baek, S. W., and Kim, M. Y., "Transient Radiative Heating Characteristics of Slabs in a Walking Beam Type Reheating Furnace," *International Journal of Heat and Mass Transfer*, Vol. 52, No. 3, 2009, pp. 1005–1011. doi:10.1016/j.ijheatmasstransfer.2008.07.030

[7] Kim, C., Kim, M. Y., Yu, M. J., and Mishra, S. C., "Unstructured Polygonal Finite-Volume Solutions of Radiative Heat Transfer in a Complex Axisymmetric Enclosure," *Numerical Heat Transfer, Part B, Fundamentals*, Vol. 57, No. 3, 2010, pp. 227–239. doi:10.1080/10407791003749134

[8] Chai, J. C., Lee, H. S., and Patankar, S. V., "Ray Effect and False Scattering in the Discrete Ordinates Method," *Numerical Heat Transfer, Part B, Fundamentals*, Vol. 24, No. 4, 1993, pp. 373–389. doi:10.1080/10407799308955899

[9] Tan, H. P., Zhang, H. C., and Zhen, B., "Estimation of Ray Effect and

False Scattering in Approximate Solution Method for Thermal Radiative Transfer Equation," *Numerical Heat Transfer, Part A, Applications*, Vol. 46, No. 8, 2004, pp. 807–829. doi:10.1080/104077890504267

[10] Coelho, P. J., "A Comparison of Spatial Discretization Schemes for Differential Solution Methods of the Radiative Transfer Equation," *Journal of Quantitative Spectroscopy and Radiative Transfer*, Vol. 109, No. 2, 2008, pp. 189–200. doi:10.1016/j.jqsrt.2007.08.012

[11] Kallinderis, Y., and Kontzialis, C., "A Priori Mesh Quality Estimation via Direct Relation Between Truncation Error and Mesh Distortion," *Journal of Computational Physics*, Vol. 228, No. 3, 2009, pp. 881–902. doi:10.1016/j.jcp.2008.10.023

[12] Zhang, H.-C., and Tan, H.-P., "Evaluation of Numerical Scattering in Finite Volume Method for Solving Radiative Transfer Equation by a Central Laser Incidence Model," *Journal of Quantitative Spectroscopy and Radiative Transfer*, Vol. 110, No. 18, 2009, pp. 1965–1977. doi:10.1016/j.jqsrt.2009.05.008

[13] Kamel, G., Naceur, B. M., Rachid, M., and Rachid, S., "Formulation and Testing of the FTn Finite Volume Method for Radiation in 3-D Complex Inhomogeneous Participating Media," *Journal of Quantitative Spectroscopy and Radiative Transfer*, Vol. 98, No. 3, 2006, pp. 425–445. doi:10.1016/j.jqsrt.2005.07.001

[14] Naterer, G. F., and Camberos, J. A., "Entropy and the Second Law Fluid Flow and Heat Transfer Simulation," *Journal of Thermophysics and Heat Transfer*, Vol. 17, No. 3, 2003, pp. 360–371. doi:10.2514/2.6777

[15] Camberos, J. A., "The Production of Entropy in Relation to Numerical Error in Compressible Viscous Flow," AIAA Fluid 2000 Symposium, AIAA Paper 2000-2333, Denver, CO, June 2000.

[16] Thomas, M. C., and Thomas, J. A., *Elements of Information Theory*, Tshinghua Univ. Press, Beijing, 2003.

[17] Camberos, J. A., "A Review of Numerical Methods in Light of the Second Law of Thermodynamics," *39th AIAA Thermophysics Conference*, AIAA, Reston, VA, 25–28 June 2007, pp. 410–444.

[18] Caldas, F., and Semiao, V., "Entropy Generation through Radiative Transfer in Participating Media: Analysis and Numerical Computation," *Journal of Quantitative Spectroscopy and Radiative Transfer*, Vol. 96, Nos. 3–4, 2005, pp. 423–437. doi:10.1016/j.jqsrt.2004.11.008

[19] Liu, L. H., and Chu, S. X., "Verification of Numerical Simulation Method for Entropy Generation of Radiation Heat Transfer in Semitransparent Medium," *Journal of Quantitative Spectroscopy and Radiative Transfer*, Vol. 103, No. 1, 2007, pp. 43–56. doi:10.1016/j.jqsrt.2006.07.004

Downloaded by HARBIN INSTITUTE OF TECHNOLOGY on April 22, 2014 | http://arc.aiaa.org | DOI: 10.2514/1.T3630